

# ON REAL-TIME SIMULATION OF THE LONGITUDINAL DYNAMICS OF TRAINS ON A SPECIFIED RAILWAY LINE

István ZOBORY and Elemér BÉKEFI <sup>‡</sup>

Department of Railway Vehicles  
Technical University of Budapest  
H-1521 Budapest, Hungary

Received: 9 November, 1994

## Abstract

The dynamical model of the train is a simplified linear lumped-parameter one. The steady-state tractive effort is specified by the points of the bivariate, control and velocity dependent tractive effort performance curves. The train is equipped with an airbrake system. The vehicles in the train are characterized by the traction resistance functions, while the railway line is specified by the arclength-dependent track-slope and track-curvature functions. The equations of motion of the train are numerically solved under real-time conditions. The drive and brake controls are given from the computer keyboard. The results of the real-time simulation can be continuously followed on the computer screen. Statistical analysis of the results and visualization can also be initiated through activating evaluation software.

*Keywords:* train dynamics, train operation, real-time simulation.

## 1. Introduction

In this paper, the train is modelled as a complex dynamical system, which moves along a specified railway line under the influence of tractive and resistance forces. The tractive influences are caused by the tractive effort exertion of the traction unit and by the track-directional components of the gravity force in case the vehicles are actually in down-hill position on the track. Resistance influences are caused on the one hand by the traction resistances, i.e. the basic resistances of the vehicles in the train and by the track-directional components of the gravity force of the vehicles that are actually in up-hill position on the track, or are positioned actually in the curved track sections, as well as by the brake application-induced braking-effort exertion, on the other. The track conditions for the considered whole railway line are specified, i.e. the inclination tangent and the radius of curvature as a function of the track arclength are numerically given by piece-wise linear functions  $\varepsilon(s)$  and  $R(s)$ . The longitudinal dynamics of

---

<sup>‡</sup>This research was supported by the Hungarian Ministry of Culture and Education, Grant No. 82/94

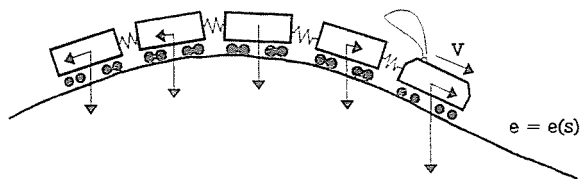


Fig. 1. Train at the peak area of a hill

a specified train operating on a specified railway line depend fundamentally on the activity of the driver, in other words, on the actual variation with time of tractive effort control function  $u_1(t)$  and the braking-force control function  $u_2(t)$ . The complex dynamical model and the motion equations, as well as the real-time simulation method will be introduced, together with the statistical evaluation diagrams of the realised operation process. The results of the investigations can be applied to the design of new traction units by utilizing the information received from the simulation of the future operation conditions on specified railway lines.

## 2. Complex Model for the Train Longitudinal Dynamics

In Fig. 1, a train is sketched, which is passing through the peak area of a hill. The vertical track profile is characterized by the function of inclination tangents vs. track-arclength  $e = e(s)$ . The gravity forces acting on the vehicles and the track-directional components of those, as well as the longitudinally sprung intervehicle connections are also shown in the Figure.

In Fig. 2, the top view of the train is shown, distances  $s_1, s_2, \dots, s_N$  between the gravity point of the locomotive and the cars in the train are also indicated. The curved track section is specified by giving the radius of curvature  $R$  and the initial and last points of the circular arc. In this way function  $R = R(s)$  (or  $1/R(s)$ ) can be determined for the whole railway line considered.

In Fig. 3, the longitudinal vibratory sub-system, i.e. the dynamical model of the train is visualized. The model is a lumped-parameter one with linear inter-vehicle springs of stiffness  $s$  and dampers of damping coefficient  $d$ . Longitudinal displacements  $x_i$ , masses  $m_i$ , rotating mass factors  $\gamma_i$ , basic resistance forces  $F_b^i$  and braking forces  $F_B^i$ ;  $i = 1, 2, \dots, N$  as well as tractive effort  $F_z$  are clearly indicated.

It should be mentioned that the basic tractive resistance forces  $F_b^i$  are velocity-dependent for non-zero velocities, while in case of zero velocity (standstill) they depend on the resultant of the non-resistance forces acting on the vehicles in question.

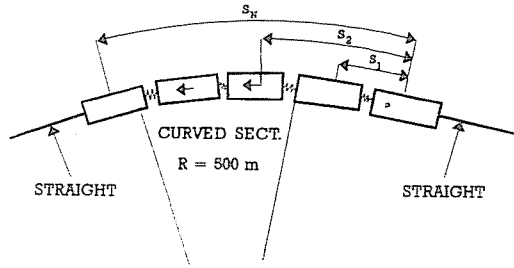


Fig. 2. Top view of the train negotiating a curve

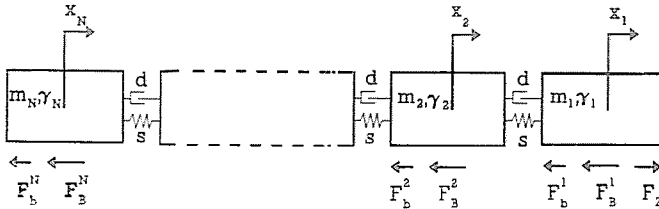


Fig. 3. The train as a longitudinal vibratory system

The tractive effort acting on the train is exerted by the locomotive situated in the front of the train. In the dynamical simulation procedure, the tractive effort is treated as a three-variate function  $F(u_1, v, t)$  which depends directly on drive control  $u_1$ , velocity  $v$  and time  $t$ . The braking-force exertion is realized vehicle-wise, i.e. regularly each vehicle in the train has its own brake-gear. The braking force is treated by using a set of three-variate functions  $F_b^i(u_2, v_i, t)$   $i = 1, 2, \dots, N$ . In the further analysis, a pneumatic brake system is dealt with, and the pneumatic transients are treated in the framework of a simplified model.

In Fig. 4, the inputs and outputs of the train as a dynamical system are visualized.

### 3. Subsystem 'Traction Resistances'

The basic traction resistance force acting on the  $i$ -th vehicle is given by formula:

$$F_b^i(v, \sum F) = \begin{cases} k(a_i v^2 + b_i |v| + c_i) \text{ sign } v & \text{if } |v| \geq \varepsilon, \\ \min\{k c_i, |\sum F|\} \text{ sign } \sum F & \text{if } |v| < \varepsilon, \end{cases} \quad (1)$$

where  $k = mg/1000$ , and  $a_i, b_i, c_i$  are vehicle-specific constants, ( $m$  is the mass of the vehicle in kg,  $g$  is the gravity acceleration in  $m/s^2$ ,  $[a_i] =$

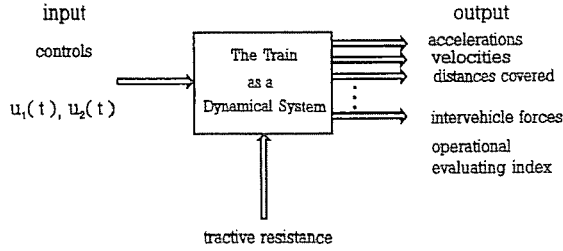


Fig. 4. Inputs and outputs of the train

$Ns^2/kNm^2$ ,  $[b_i] = Ns/kNm$ ,  $[c_i] = N/kN$ ), while  $\sum F$  is the resultant of the non-resistance forces acting on the  $i$ th vehicle (in  $N$ ). In Fig. 5 the performance surface of the bivariate function  $F_b = f(v, \sum F)$  is shown. The characteristic discontinuity of the surface over axis  $\sum F$  is very well recognizable.

In order to determine the track-directional component of the gravity force acting on the vehicle in the train, it is necessary to characterize the inclination condition of the track as a function of the track arclength. The derivative of the vertical track profile  $y(s)$  gives the tangent of inclination angle  $\alpha$ , which can be considered equal to  $\sin \alpha$  in case of small  $\alpha$  values coming into question for railway tracks. In the simulation method the track inclination will be treated in mille, i.e. instead of  $dy/ds$  the value  $\epsilon(s)\%_{\infty} = 1000 dy/ds = 1000 \operatorname{tg} \alpha$  will be taken. It is clear that the track-directional component of the gravity force can be calculated by using formula  $F_e = mg \sin \alpha \approx mgtg \alpha = mg\epsilon(s)/1000$ . If  $F_e$  is positive, its value represents the track inclination resistance, while a negative value of  $F_e$  means an additional tractive effort caused by the downhill position of the vehicle considered. The sign of  $F_e$  is uniquely determined by that of  $\epsilon(s)$ , namely in uphill position of the vehicle  $\epsilon(s)$  is positive, while in downhill position  $\epsilon(s)$  is negative. Due to this rule of signs, force  $F_e$  should be substituted into the equation of motion with a negative sign, which automatically ensures the correct mechanical conditions. In Fig. 6, the graph of function  $\epsilon(s)$  is visualized. It should be noted that in case of changing inclinations, the piecewise constant sections of  $\epsilon(s)$  will be connected by a linear transition line the slope of which is determined by the rounding circle of radius 4000 m laying in the vertical plain.

In Fig. 7, the track curvature is shown as a function of the track arclength. The curvature is positive if the curved track deviates to the right from the tangent straight line situated prior to the curve in question. The elaborated simulation method takes into consideration also the transition curves located between the straight and circular track sections.

It is assumed that the curvature in the transition curves is a linear

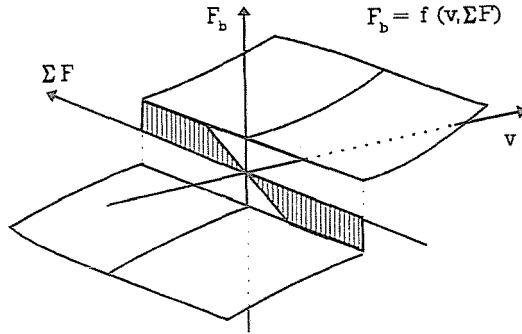


Fig. 5. Performance surface of the basic resistance force

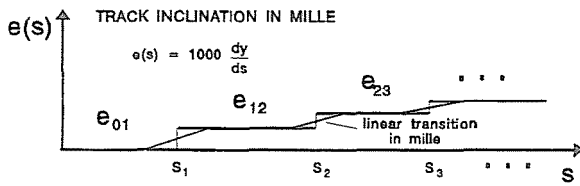


Fig. 6. Track inclination  $e$  vs. track arclength  $s$

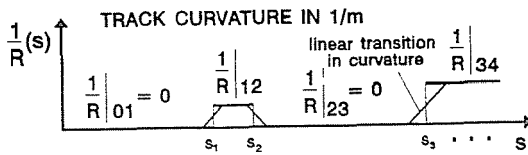


Fig. 7. Track curvature  $1/R$  vs. track arclength  $s$

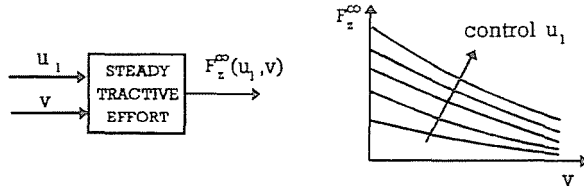


Fig. 8. Block diagram and set of stabilized tractive effort curves

function of arclength  $s$ , as it is plotted in Fig. 7. The half-length of the transition curve depends upon the radius of the circular section to be connected with the preceding or following straight section.

#### 4. Subsystem 'Tractive Effort Exertion'

The tractive effort exerted actually by the traction unit depends on the actual value of control  $u_1$ , velocity  $v$ , and due to the transients also a direct time-dependence should be reckoned with. It is to be mentioned that the time constant  $T_z$  of the transients is of order of magnitude 0.01 sec. It can be considered that for the steady-state tractive effort exertion a bivariate  $F_z^\infty(u_1, v)$  function can be taken. The values of the latter belong to the case of limit transition  $t \rightarrow \infty$ , i.e. the stabilized steady-state values are characterized. In Fig. 8, the block diagram and the set of performance curves representing function  $F_z^\infty(u_1, v)$  are shown.

If control  $u_1$  changes in a jump-like way, the tractive effort will also change but the latter change is no longer jump-like. An approximate exponential expression can be formulated for the non-steady-state tractive effort exertion as follows:

$$F_z(u_1, v, t) = F_z^* e^{-\frac{t-t_{ij}}{T_z}} + F_z^\infty(u_1, v) \left( 1 - e^{-\frac{t-t_{ij}}{T_z}} \right), \quad (2)$$

where

- $t_{ij}$  : the instant of transition in drive control function level  $u_1 = i$  to level  $u_1 = j$ ,
- $T_z$  : time constant of the tractive effort transients
- $t > t_{ij}$  : the time instant after transition point  $t_{ij}$ ,
- $F_z^*$  : the tractive effort value prevailing due to control level  $u_1 = i$  just prior to time  $t_{ij}$ ,
- $F_z^\infty(u_1, v)$  : the steady tractive effort belonging to the control level  $u_1 = j$  in case of  $t \rightarrow \infty$ .

In Fig. 9, the tractive effort transient is shown, which is caused by transition from control level  $u_1 = i$  into that of  $u_1 = j$ .

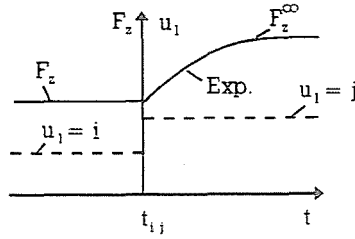


Fig. 9. Transient time function of the tractive effort in case of jump-like change in  $u_1$

### 5. Subsystem 'Braking Force Exertion'

The approximate quasi-static exponential expression for the decrease in pressure in the main pipe line as a function of time  $t$ , the instant of transition  $t_{ij}$  in control function  $u_2(t)$  and the actual pressure values  $p^*$  and  $p_{stac}$  as well as time constant  $T_f$  will be:

$$p(t) = p^* e^{-\frac{t-t_{i,j}}{T_f}} + p_{stac}(u_2) \left( 1 - e^{-\frac{t-t_{i,j}}{T_f}} \right). \quad (3)$$

In the above formula the following designations were used:

- $t_{ij}$  : the instant of transition in brake control function from level  $u_2 = i$  to level  $u_2 = j$
- $T_f$  : time constant of the pressure transient in case of brake application and release
- $t > t_{ij}$  : the time instant after transition  $t_{ij}$
- $p^*$  : the pressure value prevailing due to control level  $u_2 = i$  just prior  $t_{ij}$
- $p_{stac}(u_2)$  : the steady pressure belonging to the control level  $u_2 = j$  in case  $t \rightarrow \infty$
- $p_0$  : maximum pressure level in the main brake pipe-line
- $p_m = p_0 - p$  : the actual pressure in the main brake pipe-line; in case of the  $i$ th vehicle a signal propagation retardation  $\tau_i$  should be reckoned with  $p_m^i(t) = p_0 - p(t - \tau_i)$ ,  $i = 1, 2, \dots, N$ .
- $p_c^i$  : the brake cylinder pressure at the  $i$ th vehicle:  $p_c^i(t) = Kp(t - \tau_i)$ , where  $K$  is constant.

In Fig. 10, the brake cylinder pressure vs. time functions are plotted for the locomotive ( $p_c^1$ ) and for the  $i$ -th car ( $p_c^i$ ). The time shift  $\tau_1$  due to the pressure signal propagation velocity is clearly indicated.

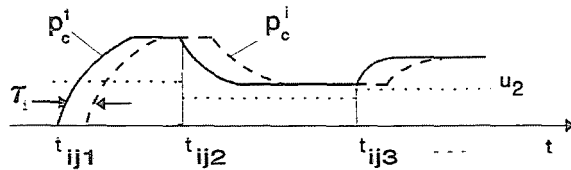


Fig. 10. Cylinder pressure vs. time functions

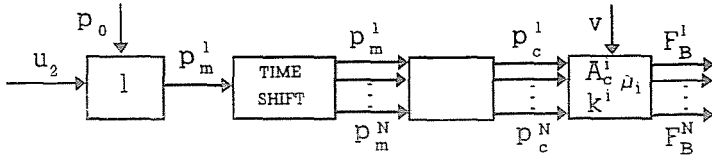


Fig. 11. Flowchart of the braking force exertion

The total brake-block force acting on the  $i$ th vehicle can be computed by the following formula:

$$F_t^i = p_c^i A_c^i k^i, \quad (4)$$

where  $A_c^i$  is the area of the brake cylinder cross-section and  $k^i$  is the torque ratio (mechanical advantage) of the brake leverage for the  $i$ th vehicle. With the knowledge of the virtual friction coefficient function  $\tilde{\mu}^i(p_b^i, v^i)$  belonging to the brake-block wheel tread friction connection, the braking force acting on the  $i$ th vehicle can be computed by the following formula

$$F_B^i = F_t^i \tilde{\mu}^i(p_b^i, v^i), \quad i = 1, 2, \dots, N. \quad (5)$$

In the formula,  $p_b^i$  stands for the actual value of the brake-block pressure, while  $v^i$  is the velocity of the  $i$ th vehicle.

The flowchart of the braking-force exertion is shown in Fig. 11. Brake control  $u_2$  and pressure  $p_0$  in the main air reservoir of the locomotive determine the main pipeline pressure  $p_m^1$  in the locomotive, from which the appropriate pipeline pressures  $p_m^i$ ;  $i = 2, 3, \dots, N$  can be determined by using the time-shifts mentioned above. With the knowledge of the pipeline pressure time functions for each vehicle in the train, also the time functions of the brake-cylinder pressure can be determined by taking into consideration the approximate proportional and 'counter-tact' variation character of the pipeline and brake-cylinder pressures.

## 6. Subsystem 'Unified Resistance Forces'

The basic traction resistance force, the curving resistance force and the braking force are originated from certain torque effects influencing the motion

of the wheelsets. The peripheral force corresponding to some of the torques mentioned above can be considered as the 'unified resistance force'.

The 'unified' resistance force  $F_{bRB}$  (in N) can be computed by using the train of thoughts similar to that described in case of traction resistances. The formula has the following form:

$$F_{bRB} = \begin{cases} \min\{|F_a(v)|; K(av^2 + b|v| + c) + \\ + |F_R| + |F_B|\} \text{ sign } v & \text{if } |v| \geq \varepsilon \\ \min\{|\sum F|, \min\{|F_a(0)|, Kc + \\ + |F_R| + |F_B(0)|\}\} \text{ sign } \sum F & \text{if } |v| < \varepsilon \end{cases}, \quad (6)$$

where the following designations were used:

- $v$  : the velocity of the vehicle in m/s  
 $F_a(v)$  : the maximum adhesion force transmittable in the wheel-rail connection without macroscopic sliding as a function of travelling velocity ( $[F_a] = \text{N}$ )  
 $K$  :  $\text{mg}/1000$  the weight of the vehicle in kN  
 $a, b, c$ : coefficients of the quadratic specific basic traction resistance vs. velocity function.  $[a] = \text{Ns}^2/\text{mkN}$ ,  $[b] = \text{Ns}/\text{mkN}$ ,  $[c] = \text{N}/\text{kN}$   
 $\sum F$  : the resultant of the non-resistance forces acting on the vehicle at zero velocity, i.e.  
  - tractive effort exerted by the drive system,
  - track-directional component of the gravity force and
  - forces acting on the vehicle through the buffer and drive-gears from the adjacent vehicles $F_R$  : the curve resistance force acting on the vehicle in N  
 $F_B$  : the braking force acting on the vehicle in N  
 $F_a(0)$  : limit value of the maximum adhesion force at zero velocity in N  
 $F_B(0)$  : limit value of the braking force at zero velocity in N

It should be noted that  $F_B$  depends on velocity  $v$  and actual brake control  $u_2$ , while  $F_B(0)$  also depends on  $u_2$ . Curving resistance force  $F_R$  depends upon the distance covered by the vehicle ( $s$ ). The force values building up  $\sum F$  can also depend on the distance covered by the vehicle in question and due to the longitudinal connection forces (transmitted by the draw-gears and buffer-gears from the adjacent vehicles), forces  $\sum F$  can depend on distance covered  $s_1, s_2$  and velocities  $v_1, v_2$  of the adjacent vehicles, respectively. In addition, in case of a traction unit,  $\sum F$  can depend also on the actual drive control  $u_1$ . In this way, in a general case the unified resistance force has eight independent variables as indicated in the following expression:

$$F_{bRB} = f(s, v, \sum F(s_1, v_1, s, v, s_2, v_2, u_1), u_2). \quad (7)$$

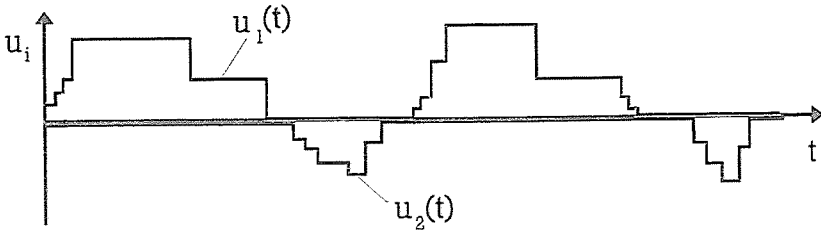


Fig. 12. Characteristic pair of drive and brake control functions

Formula (7) shows the complicated structure of the unified resistance force introduced in (6).

### 7. Simulation in the Time Domain Controls from the Keyboard

Control functions  $u_1(t)$  (drive control) and  $u_2(t)$  (brake control) are the inputs of the system to be simulated, and in our model both functions are step functions taking finite number of integer values due to the following definitions:

$$\begin{aligned} u_1(t) &\in \{0, 1, 2, \dots, 15\} \\ u_2(t) &\in \{0, -1, -2, \dots, -15\} \end{aligned}$$

Control functions in question are plotted in Fig. 12.

The integers representing the possible levels to be taken by the control functions are corresponding to keyboard positions (buttons), chosen in an appropriate way. If one pushes a keyboard button, the control takes an integer value belonging to the position in question, and its value remains unchanged up to the subsequent pushing of any other keyboard button assigned for the possible values of the control function in question. The partition of the keyboard positions used by the authors is shown in Fig. 13.

The mathematical description of the train motion in a specified complex environment is carried out by using a set of non-linear differential equations. If the number of vehicles in the train is  $N$  (i.e. mechanical system with  $N$  degree of freedom is dealt with) then the state vector is of  $2N$  dimension. State vector  $\mathbf{Y}$  contains the velocities in coordinates  $1, \dots, N$ ; and the displacements in coordinates  $N + 1, \dots, 2N$ . The set of motion equations written for state vector  $\mathbf{Y}(t)$  has the following form:

$$\dot{\mathbf{Y}} = \mathbf{A}\mathbf{Y} + F(\mathbf{Y}, u_1, u_2, t), \quad (8)$$

where  $2N \times 2N$  coefficient matrix  $\mathbf{A}$  is the so-called system matrix, which

```

BRAKE      1  2  3  4  5  6  7  8  9  0
CONTROL    [1][2][3][4][5][6][7][8][9][0]
POSITIONS  [Q][W][E][R][T][Y]
           10 11 12 13 14 15

DRIVE      1  2  3  4  5  6  7  8  9
CONTROL    [A][S][D][F][G][H][J][K][L]
POSITIONS  [Z][X][C][V][B][N][M]
           10 11 12 13 14 15  0
    
```

Fig. 13. Brake and drive controls from keyboard

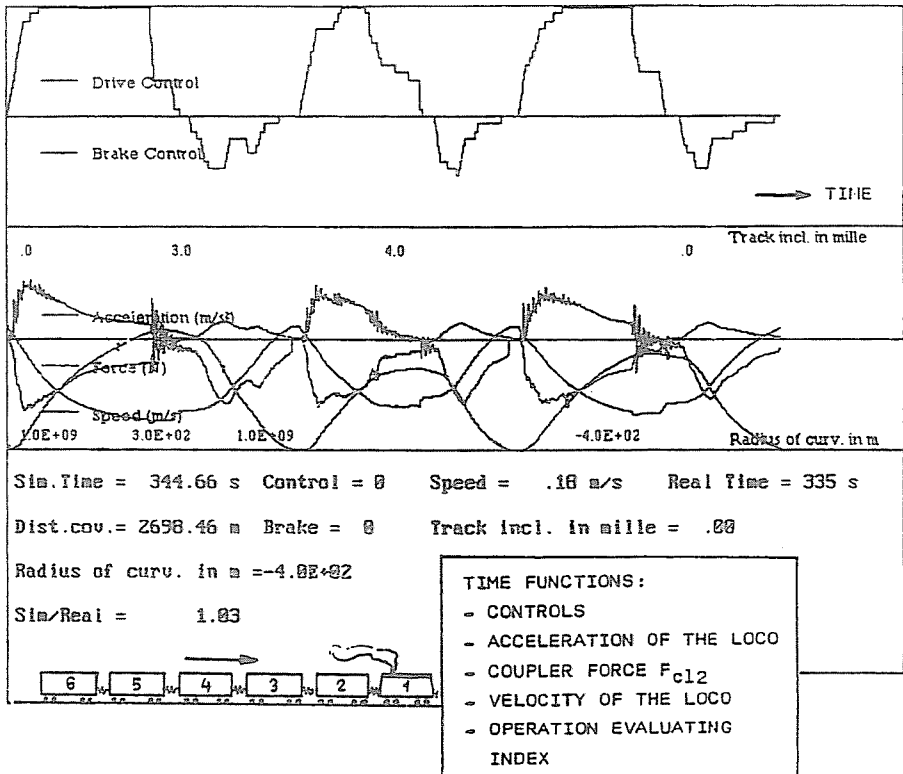


Fig. 14. Diagrams and numerical information on the computer screen

has the following special structure:

$$A = \begin{bmatrix} -M^{-1}D & -M^{-1}S \\ E & 0 \end{bmatrix}. \quad (9)$$

In the expression of matrix **A**, **S** is the  $N \times N$  stiffness matrix, **D** is the  $N \times N$  damping matrix, **M** is the  $N \times N$  mass matrix, **E** is the  $N \times N$  unit matrix

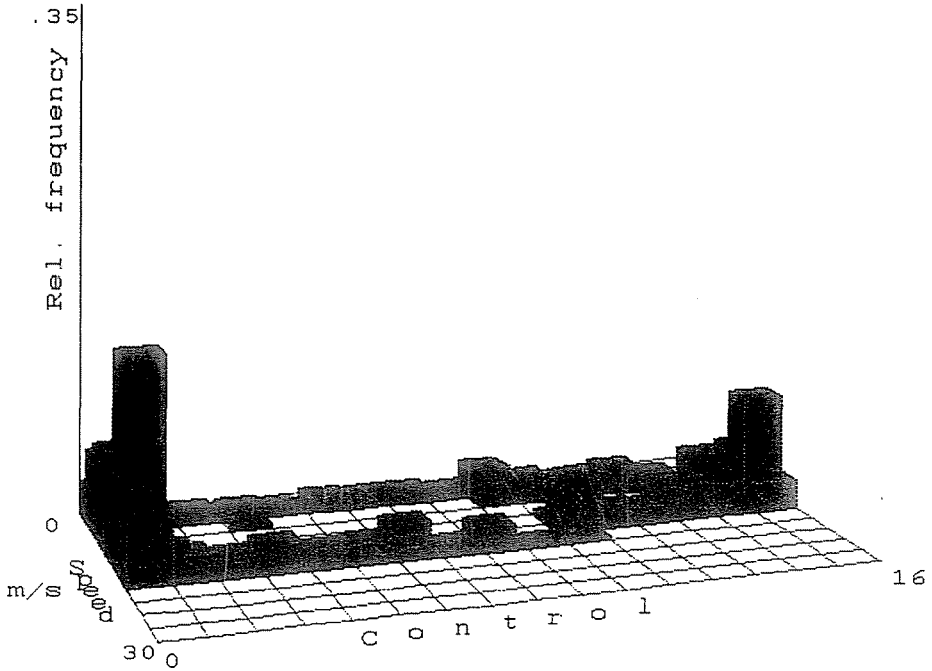


Fig. 15. Joint distribution of the drive control and speed

while  $\mathbf{0}$  is the  $N \times N$  zero matrix. Vector-valued function  $\mathbf{F}(\mathbf{Y}, u_1, u_2, t)$  is of a very complicated structure and is strongly non-linear. The set of motion equations is to be solved numerically (Euler's method, Rung-Kutta method, etc.) Characteristic time step for the real-time simulation is of  $\Delta t = 0.01$  sec order of magnitude.

The set of diagrams displayed on the computer screen is shown in Fig. 14. The control functions, the acceleration and velocity functions of the locomotive, as well as the time function of the coupler force arising in the draw and buffer gear of the locomotive, and that of the operational evaluation index can clearly be identified. In the lower part of the Figure the numerical information characterizing the simulation process is visible.

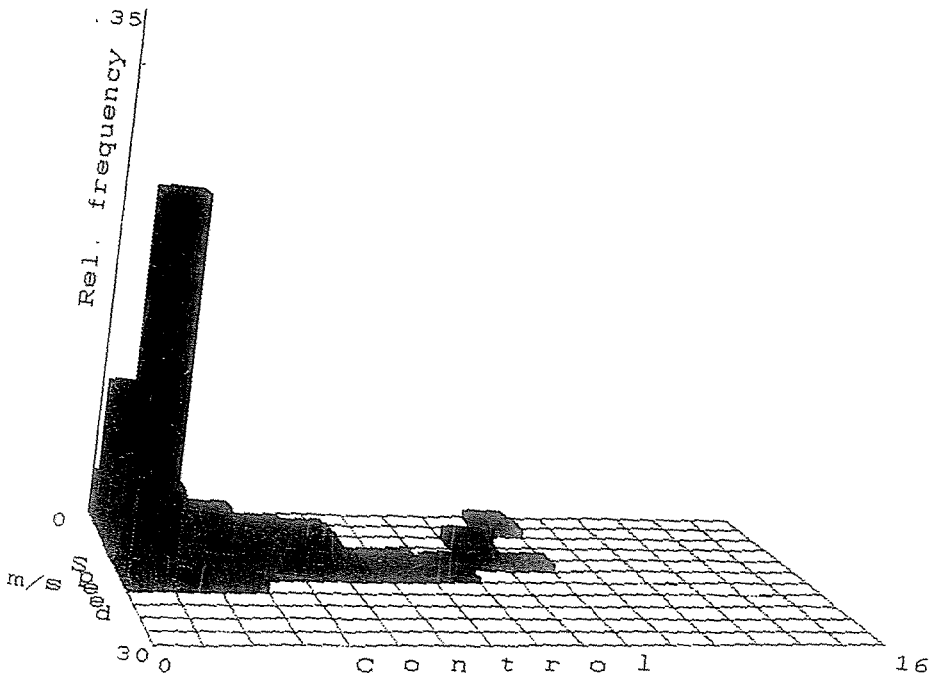


Fig. 16. Joint distribution of the brake control and speed

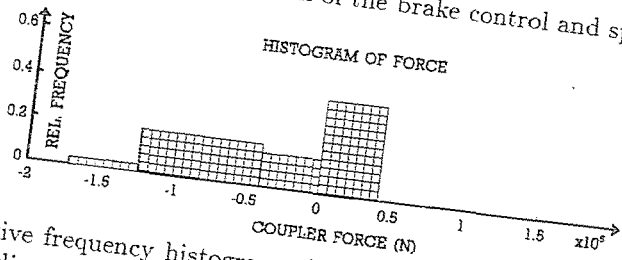


Fig. 17. Relative frequency histogram of the coupler force between the loco and the adjacent carriage

### 8. Statistical Evaluation of the Responses

In the course of the simulation procedure the relative frequencies of certain events are continuously computed. The events in question are defined by using a partition of the ranges of the state vector coordinates and other state dependent quantities, as well as the controls.

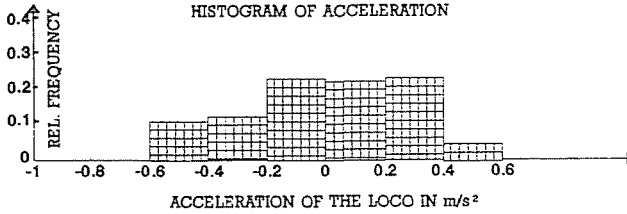


Fig. 18. Relative frequency histogram of the loco's acceleration

For the sake of visualization, joint probability distribution of the drive control and the locomotive velocity  $\mathbf{P}\{u_1 \in \Delta u_i, v_{\text{loco}} \in \Delta v_j\}$  is approximated by determining the relative frequency histogram shown in Fig. 15. The joint probability distribution of the brake control and the locomotive velocity  $\mathbf{P}\{u_2 \in \Delta u_i, v_{\text{loco}} \in \Delta v_j\}$  is treated in a similar way in Fig. 16. The simulated coupler force between the locomotive and the first carriage, as well as the acceleration process of the locomotive were also evaluated by determining relative frequency histograms, which approximate to probability distributions  $\mathbf{P}\{F_{cl2} \in \Delta F_i\}$  and  $\mathbf{P}\{a_{\text{loco}} \in \Delta a_i\}$ , respectively. The diagrams are plotted in Figs. 17 and 18.

The relative frequency distribution can be used in the course of designing the drive system components, e.g. the roller bearings, the gear-wheels and the shafts, as well as the components of the brake gear, e.g. the linkages and the leverages. The knowledge of the relative frequencies belonging to the different loading conditions makes it possible to carry out dimensioning procedures taking into consideration the fatigue phenomena.

## 9. Concluding Remarks

The investigations of the authors into the longitudinal dynamics of trains in complex environment, the elaboration of the simulation models and programs and real-time simulations carried out made it possible to summarize the following statements:

- The real-time simulation of the train longitudinal dynamics can be carried out by using simplified dynamical model and approximate process description for the airbrake system.
- The continuous simulation requires the unified treatment of the resistance forces acting on the vehicles.
- The numerical integration in the real-time simulation requires a time step of order of magnitude 0.01 sec.
- The elaborated simulation procedure makes it possible to predict the loading conditions of the components built into the vehicle's structure and the drive/brake system already *in the period of the vehicle design*.

- The predictions mentioned appear in the form of probability approximating relative frequency distributions and further statistical parameters.
- The simulation procedure can yield also values characterizing the energy consumption and environment pollution characteristics of the vehicle realized in the course of the operation process.

### References

- [1] ZOBORY, I.: Stochasticity in Vehicle System Dynamics. *Proceedings of the 1st Mini Conference on Vehicle System Dynamics, Identification and Anomalies*. Held at the TU of Budapest, 1988, pp. 8-21.
- [2] ZOBORY, I.: Prediction of Operational Loading Conditions of Powered Bogies. *Vehicles, Agricultural Machines*, 1990. Vol. 37, Issue 10, pp. 373-376 (in Hungarian).
- [3] MICHELBERGER, P. - ZOBORY, I.: Loading Conditions of Ground Vehicles in Operation. *Proceedings of the 2nd Mini Conference on Vehicle System Dynamics, Identification and Anomalies*. Held at the TU of Budapest, 12-15 of November 1990, pp. 246-262.
- [4] MICHELBERGER, P. - ZOBORY, I.: Operation Loading Conditions of Ground Vehicles - Analysis of Load History. *Proceedings ASME Winter Annual Meeting*, Dallas, New York, 1990, pp. 175-182.
- [5] HORVÁTH, K. - ZOBORY, I. - BÉKEFI, E.: Longitudinal Dynamics of a Six-unit Metro Train-set. *Proceedings of the 2nd Mini Conference on Vehicle System Dynamics, Identification and Anomalies*. Held at the TU of Budapest, 12-15 of November 1990, pp. 45-62.
- [6] ZOBORY, I. - FRANG, Z. - SZABÓ, A. - GYÖRIK, A.: Investigation of Operation Loading Conditions of Electric Locomotive of Series V43. *Review of Transportation Sciences*. Volume XLI. Issue 6. Budapest, 1991, pp. 201-215 (in Hungarian).
- [7] ZOBORY, I. - BÉKEFI, E.: Software for Stochastic Simulation of Motion and Loading Processes of Vehicles. *Proceedings of the 3rd Mini Conference on Vehicle System Dynamics, Identification and Anomalies*. Held at the TU of Budapest, 9-11 of November, *Periodica Polytechnica, Transportation Engineering*, Vol. 22, No. 2, pp. 111-127, 1994.
- [8] ZOBORY, I.: Stochastic Simulation of the Motion and Loading Processes of Railway Traction Units. *Review of Transportation Sciences*, Vol. XLII, Issue 1, Budapest, 1993, pp. 19-29 (in Hungarian).